# Measurement of rolling resistance and scrub torque of manual wheelchair drive wheels and casters
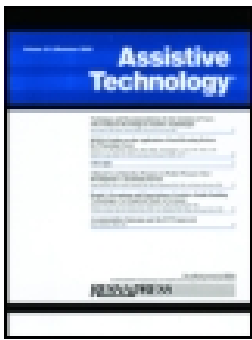
**3 authors**, including:

Jacob Misch
Georgia Institute of Technology
**4** PUBLICATIONS **7** CITATIONS

# Measurement of rolling resistance and scrub torque of manual wheelchair drive wheels and casters

Stephen Sprigle, Morris Huang & Jacob Misch

Taylor & Francis
Taylor & Francis Group

Check for updates

# Measurement of rolling resistance and scrub torque of manual wheelchair drive wheels and casters

Stephen Sprigle, PhD, PT ⬥, Morris Huang, PhD, and Jacob Misch, BSME

Rehabilitation Engineering and Applied Research Lab, Georgia Institute of Technology, Atlanta, Georgia, USA

## ABSTRACT

The effort needed to maneuver a manual wheelchair is a function of the occupied wheelchair's inertia and energy loss. The primary source of energy loss is due to the resistance of the drive wheels and casters on the ground. Specifically, manual wheelchairs have two major sources of frictional energy loss: rolling resistance and scrub torque. The objective of this study was to develop and validate component-level test methods to evaluate the energy loss properties of drive wheels and casters on different surfaces and with different applied loads. Rolling resistance is measured using a weighted coast-down cart and scrub torque is calculated by measuring the force required to rotate a plate that is loaded onto the tire's surface. Each test method was iterated and then applied to a cohort of drive wheels and casters. Both test methods demonstrated acceptable repeatability and the ability to distinguish energy loss parameters between common wheelchair components. The results show that caster and drive wheel energy losses can vary significantly across surfaces and with increased load on the casters. However, the findings also illuminate complex relationships between rolling resistance and scrub torque performance that embody a tradeoff in performance as applied to mobility during everyday life.

## Introduction

As with any other mechanical system, manual wheelchair (MWC) components determine its mechanical performance. The composite mass and inertia of the wheelchair frame, casters, drive wheels, and other components dictate the effort with which the MWC system can change speed and direction. Energy losses due to surface interactions, frame flexion, and vibrations can lead to increased propulsion effort while maneuvering.

In MWCs, the tires can be considered as the strongest determinants of system energy loss because they dictate surface interactions. When compared to other human-propelled wheeled vehicles such as the bicycle, the MWC is distinct because it operates at much lower velocities (Sonenblum & Sprigle, 2016), which diminishes its sensitivity to vibrational loss and air drag. Experimental and modeling wheelchair literature lend support that drag and bearing loss contributions can be considered negligible (Hofstad & Patterson, 1994), which leaves casters and drive wheels as the predominant sources of loss for MWCs.

Energy losses due to wheels and casters have motivated a fair amount of research, which has typically focused on rolling resistance. Some studies used loaded or occupied wheelchairs to measure system-level energy losses (Chan, Eshraghi, Alhazmi, & Sawatzky, 2018; Hoffman, Millet, Hoch, & Candau, 2003; Lin, Huang, & Sprigle, 2015; Sawatzky, Kim, & Denison, 2004; Zepeda, Chan, & Sawatzky, 2016). These approaches, however,

do not allow for the independent assessment of caster and drive wheel performance. The rolling resistances of drive wheels have been directly measured using treadmills (Frank & Abel, 1989) and rollers (Kwarciak, Yarossi, Ramanujam, Dyson-Hudson, & Sisto, 2009). The use of these methods, however, limits the surfaces that can be evaluated. Over-ground methods, on the other hand, can study different surfaces, but have other technical and operational challenges.

Characterizing the rolling resistance of casters and drive wheels reflects energy losses during purely rectilinear motion. However, turning maneuvers are ever-present in wheelchair mobility (Sonenblum, Sprigle, & Lopez, 2012). Few studies have ventured to characterize the turning resistances of maneuvering wheelchairs as a system (Bascou et al., 2014; Bascou, Sauret, Villa, Lavaste, & Pillet, 2015; Lin et al., 2015), or individual MWC components (Kauzlarich, Bruning, & Thacker, 1984). Frank and Abel examined the resistive losses of casters in terms of their scrub torque, which is the resistance experienced by the wheel when pivoting without rolling (Frank & Abel, 1989). This torque can be likened to the resistance experienced when one dry-steers in an automobile. Two recent studies (Silva, Corrêa, Eckert, Santiciolli, & Dedini, 2017; Silva, Dedini, Corrêa, Eckert, & Becker, 2016) have empirically measured and modeled the cornering force present in MWC drive wheels, a resistive force that manifests itself when the MWC undergoes turns with a non-zero radius of curvature which involves the wheels simultaneously rolling and turning. These prior approaches are important because

Color versions of one or more of the figures in the article can be found online at www.tandfonline.com/UATY.
Supplemental data for this article can be accessed on the publisher's website.

they seek to characterize an important performance parameter: energy loss during turning.

The objective of this study was to develop and validate component-level test methods to evaluate the energy loss properties of manual wheelchair drive wheels and casters. These test methods were designed to assess energy loss on different surfaces and, collectively, reflect performance in straight and turning trajectories. As such, two component-level tests were developed and validated which targeted rolling resistance force and scrub torque. These methods were iteratively developed and validated by assessing the performance of a small cohort of casters and drive wheels.

## Description and validation of a coast-down method to measure rolling resistance

### System design and rationale

The functional design requirements for measuring rolling resistance were defined as: 1) the technique must measure both casters and drive wheels, 2) the instrumentation does not impact the tested component inertias and resistive forces, 3) the test can be deployed on different surfaces, and 4) the space requirements are reasonable and compatible with typical hallways.

These requirements led to the design of a coast-down cart method that utilizes four design features: a platform capable of supporting loads representing an occupied wheelchair, multi-axle mounts, wheel "encoders", and "reference" cart wheels.

The body of the coast-down cart (Figure 1) was constructed with a 41 cm x 71 cm sheet of plywood, with a 3/4" thickness to support a mass of 100 kg. The front axle mounts were designed to accommodate a single pair of casters to serve as "reference" wheels for all tests. In this study, a pair of commonly available Primo 6 × 1.5" casters (Pr1mo HPW-170's, Primo Latinoamerica, Xiamen, China) was used as a reference. Rear axle mounts were designed for mounting the "test" drive wheels and casters of various sizes. The heights of the rear axle holes were defined such that when a set

of "test" wheels was mounted, the cart surface remain horizontal (design requirement was ≤2 degrees). The use of 6" dia casters as reference wheels allowed the cart to be designed to accommodate both smaller casters and larger drive wheels while providing adequate surface area upon which to mount the accelerometer.

The cart design allows for investigation of rolling resistance as a function of the weight on the test wheels and casters. Weight distribution was calculated using the cart's fore-aft center of mass (COM) and its axle-to-axle distance. Within this study, COM was measured using the iMachine (Eicholtz, Caspall, Dao, Sprigle, & Ferri, 2012), a device designed to measure the inertias of loaded wheelchairs, but other techniques can be used.

Front caster velocity was measured using time-synchronized 3-axis accelerometers (MSR Electronics, Seuzach, Switzerland) that are mounted to the face of each of the "reference" wheels (Figure 1), such that one axis is aligned with and centered on the axle. Each accelerometer was set to sample at the maximum rate of 51.2 Hz. Accelerometers were selected because they act as simple and affordable encoders by tracking the angles of their coordinate axes relative to gravity. The angular position of the wheel is calculated using the inverse tangent of the accelerations of the wheel's planar axes which is then differentiated to calculate the wheel's angular velocity. Accuracy of using accelerometers for this purpose was done using a digital encoder (US Digital, Vancouver WA) which found the accelerometer data to have an average absolute error of 1.76%.

The wheel angular velocity derived from these accelerometers was then coupled with dimensional measurements of the "reference" wheels to determine the velocity of the cart and to assess the quality of the maneuver. Equations (1–2) define the velocity of the cart at the center of the front axle, and the cart's yaw rate. The $v_{AC}$ is the cart front axle center velocity, $\dot{\psi}$ is the cart yaw (turning) rate, $r$ is the "reference" (front) wheel radii, $s$ is the lateral wheel base of the "reference" wheels, and $\dot{\phi}_L$ and $\dot{\phi}_R$ are the left and right "reference" wheel angular velocities.
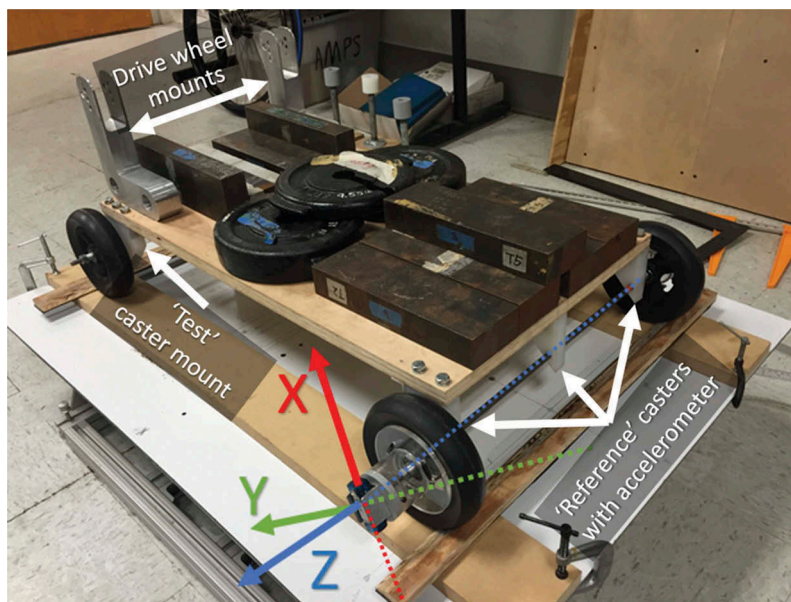


**Figure 1.** Coast-down cart frame.

$$v_{AC} = r\left(\frac{\dot{\phi}_L + \dot{\phi}_R}{2}\right) \tag{1}$$

$$\dot{\psi} = r\left(\frac{\dot{\phi}_R - \dot{\phi}_L}{s}\right) \tag{2}$$

Because the weight on the reference wheels can minimally alter their active radii, this parameter is measured for each test configuration using a caliper. Yaw rate is considered as a means to ensure the cart tracks in a straight trajectory using the relative velocities of the right and left reference wheels. Successful trials were defined when the heading changed ≤ degrees within the analysis window.

The protocol used an analysis window of 0.95 m/s to 0.65 m/s – defined based on typical speeds of wheelchair users measured during everyday mobility (Sonenblum et al., 2012). Cart velocities are plotted and a linear regression is fit to this segment and the slope of the line is taken as the average deceleration rate as shown in Figure 2. The measured response demonstrated high linearity with typical $R^2$ values exceeding 0.99. To meet this analysis window, the methodology calls for the cart to be pushed to reach a release speed between 1.0 and 1.2 m/s. This approach also reduces the spatial requirements of the test because the cart can be stopped manually, well before it coasts to a complete stop.

Having described all the parameters and methods necessary to evaluate the cart's coast-down deceleration, the final step is to translate this deceleration rate into rolling resistance force. To calculate the rolling resistance force of the "test" wheels, the resistance force of the system's reference wheels must be measured. By loading a cart fitted with four identical "reference" wheels with a 50–50 fore-aft weight distribution, the rolling resistance force of a single "reference" wheel can be described by Equation (3):

$$(F_{RR})_{ref} = \frac{Ma_{cart}}{4} \tag{3}$$

where $(F_{RR})_{ref}$ is the rolling resistance force of a single "reference" wheel, $M$ is the total mass of the loaded cart system, and $a_{cart}$ is the deceleration of the cart. When the cart is equipped with two "test" wheels, $(F_{RR})_{ref}$ is subtracted to calculate the rolling resistance force on the "test" (rear) wheels using Equation (4):

$$(F_{RR})_{test} = \frac{Ma_{cart} - 2(F_{RR})_{ref}}{2} \tag{4}$$

where $(F_{RR})_{test}$ is the rolling resistance force of a single "test" wheel.

### System validation

Test repeatability was defined based on the benchmark of a coefficient of variation (CV) <10% for deceleration rates measured across 10 repeated trials.

Tests were conducted on a defined segment of level ground in both the "forward" and "backward" heading directions along this track. The resulting deceleration values of the two directions were averaged and used to calculate rolling resistance force. This approach is needed to accommodate surface irregularities such as floor slope.

Test repeatability was characterized for every coast-downs trial set. For each unique combination of cart load, "test" wheel, surface, and track direction, a series of 15 repeated coast-down trials were performed. From this series, a trial set of 10 were selected based on whether their release velocities fell within the 1.0–1.2 m/s range and met the straight heading requirement.
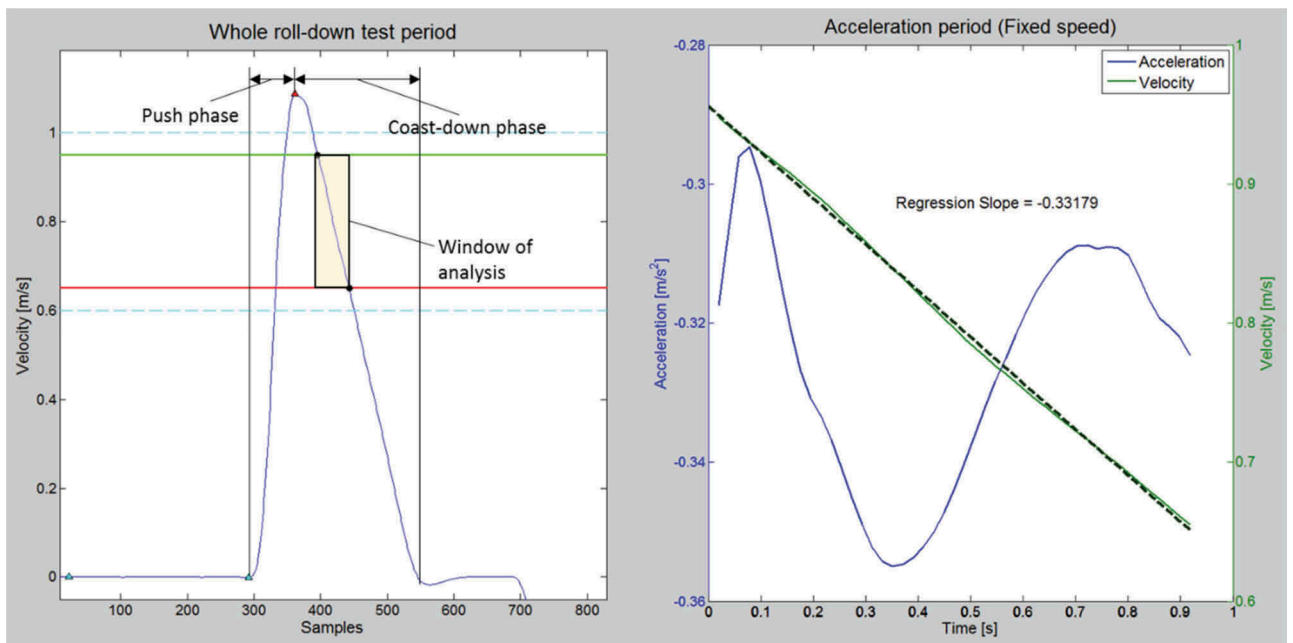


**Figure 2.** Velocity profile of a single coast-down. Left: plot of velocity during entire trial indicating the analysis window of 0.95 m/s (green) to 0.65 m/s (red). Right: acceleration and velocity plots and including the regression line used to define deceleration.

# Development of wheel scrub method

## Test method rationale

We elected to characterize the scrub torque of the casters and drive wheels with zero radius of curvature instead of their corner force. While measuring cornering forces would better represent curvilinear MWC maneuvers, there was a three-fold rationale for this decision: 1) the scrub torque represents an upper bound on the turning resistance a component would experience at a given load, 2) an infinite number of turning radii can be evaluated to describe turning force, so any choice would inherently include tradeoffs, and 3) the scrub torque measurement methodology was significantly more simplistic, which is an important factor in developing an accessible test method.

Design criteria included the ability to measure scrub torque 1) directly on the drive wheels and casters using the same technique, 2) on different surfaces, and 3) using different loads.

## System design

The scrub torque measurement test applies a normal load to a surface–wheel interface, and then measures the force required to rotate a surface contact plate. The relative motion between the test surface and wheel emulates the wheel scrubbing (pivoting) on the test surface. The overall apparatus can be divided into three modular parts: 1) the pull force actuator, 2) the wheel mounting and loading frame, and 3) the surface loading post (Figure 3).

The pull force actuator module incorporates a materials-testing system (Zwick-Roell, Ulm, Germany) to make use of its linear actuator, load cell, and data acquisition software (testXpert II). A pulley is mounted on a height-adjustable frame under the load cell and is responsible for translating the vertical pull force into a horizontal pull force via a cable.

Both drive wheels and casters must be secured during the test. The mounting frames accept axles and use spacers to prevent lateral motion. Caster rotation was constrained using plungers that contact the lateral aspects of the wheel. Drive wheel rotation was constrained using repurposed MWC wheel locks. Scrub test patches were documented before each test and the wheel was rotated between trials to prevent overuse of any particular tire patch.

The surface loading post is comprised of a loading platform, cable spool, and surface mounting plate. The loading platform is a circular Dibond aluminum composite disk designed to support multiple standard plate weights and is connected to a 1.5” diameter vertical aluminum load arm. A length of 1/2” diameter steel rod connects the load arm to the cable spool, which is configured with an internal bearing to decouple the spool rotation from the loading platform. Thus, when a pulling motion is applied to the cable, the spool and surface mounting plate rotate to scrub against the wheel while the loading plate remains stationary. The 5” x 5” surface mounting test plate was designed to accommodate the largest contact patch of the drive wheels when loaded. The test surface material (i.e., tile or carpet) were epoxied to these plates. The Zwick cross-head is lowered to the start position and the cable is spooled without load on the test plate such that, after load is applied, the cable length between the pulley and spool is horizontal and tangent from the spool when taut (Figure 3). For each scrub test, the pull rate of the linear actuator is 5 cm/s for a total pull length of 38 cm. Since the spool diameter is 6.41 cm, the linear motion equates to a rotational rate of 1.56 rad/s (a quarter revolution per second) and a total rotation of 11.85 radians (or 1.89 revolutions) for the test surface. This rotational rate was selected based on previously observed rates of MWC turning
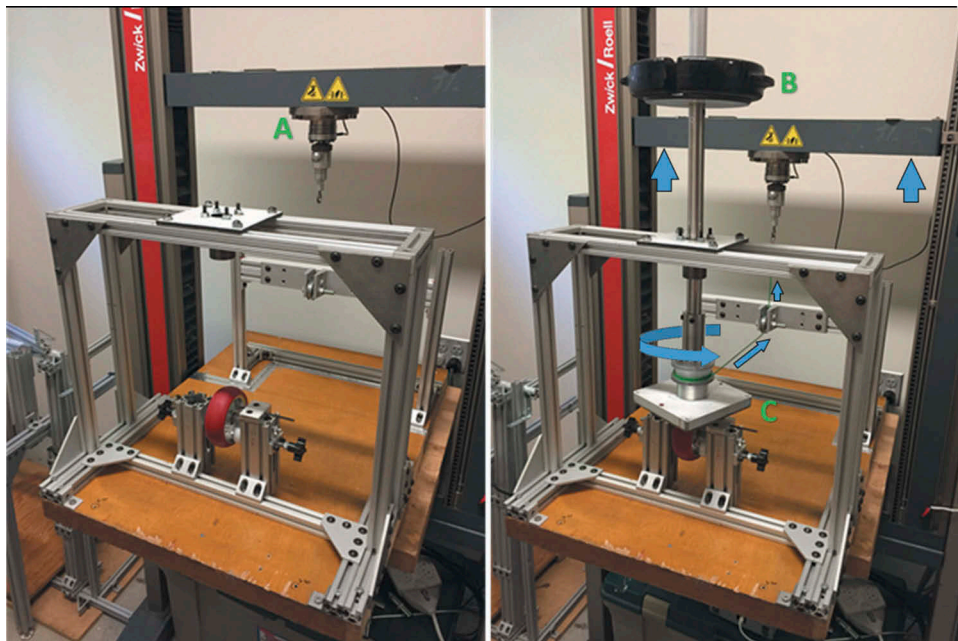

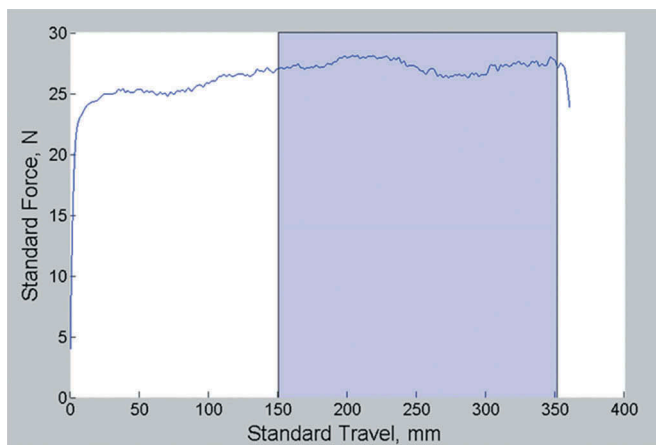
**Figure 3.** Scrub test rig design.

**Figure 4.** Caster scrub test pull force data.

(Sonenblum et al., 2012), while the rotational displacement was selected to capture at least one revolution of steady-state scrub torque.

The collected load cell pull force data and the corresponding actuator linear displacement were collected at a sampling rate of 100 Hz. The selected window of analysis was from 150 mm to 351 mm of the linear actuator displacement. The window from 0 mm to 149 mm removes slack in the cable and accommodates for any transitional inconsistencies as the contact surfaces reach a steady-state interaction. Thus, the steady-state scrub torque is captured from 150 mm to 351 mm as illustrated by the shaded region in Figure 4. The force data within this window were averaged and multiplied by the spool diameter (6.41 cm) to yield the scrub torque for that trial.

Before testing, the surface of the test wheel is cleaned and one trial is performed at the specified test weight to "condition" the wheel patch. This conditioning methodology shares consistency with ASTM standards (D1349-14 A, 2014; E1337-90 A, 2012) for measuring auto tire braking resistance and evaluating rubber material friction. To characterize scrub torque for a single load, a set of 5 repeated trials are performed and the results are averaged to give the representative value for that caster under that load and surface configuration.

### System validation

One design specification of this system requires assurance that the pull forces do not impact the vertical loading during the test. Applied force accuracy and consistency was tested using a Shimpo FG-3008 force gage (Nidec-Shimo Corp., IL) mounted under the surface mounting plate. Over the respective range of loads, vertical force throughout the test was very consistent with a CV ≤1%. Loading was accurate at the start and end of the test and varied <1% for casters and <2% for drive wheels.

The repeatability of each scrub test rig was assessed with the benchmark of CV < 10% for a set of 5 repeated trials. Initial testing confirmed the need for pre-conditioning trials to establish a more consistent testing surface.

### Component testing

A diverse set of casters and drive wheels were selected for testing. All components represented options that are available for configuring ultra-lightweight wheelchairs. A range of designs was sought to embody a valid representation of the diversity in commercial wheelchair components. Additionally, the ability to test a range of components is necessary for the development of a robust test methodology.

Each of the wheelchair casters and drive wheels were acquired brand new for testing. The unloaded diameter, tire width, and profile of each caster and drive wheel were measured. A digital scale was used to measure mass. Tire hardness was measured using a Type A durometer (Shore Instrument & Mfg. Co., NY). All measurements of pneumatic casters and wheels were taken with their inner tubes inflated to the recommended pressure. Drive wheels that were provided with a range of recommended pressures were tested at 100 psi, which was within the recommended range. The comprehensive properties of each caster and drive wheel are described in Tables 1 and 2, respectively. The wheel profile outlines in Figure 5 further illustrate the diversity of the shapes and sizes of the tested components.

### Testing protocol

Components were tested using three different loads and on two surfaces to characterize performance under different contexts of use. The loading conditions were based on the framework of an occupied MWC with a 100 kg mass which is consistent with wheelchair standards (International Standards Organization) and configured at three distinct weight distributions: 60%, 70%, and 80% load on the drive (rear) wheels. These weight distributions were based upon clinical relevance and related literature (Brubaker, 1986; Lin & Sprigle, 2019; Sawatzky et al., 2004). Thus, the casters and drive wheels were loaded at three magnitudes for each of the component tests (Table 3). Two test surfaces were selected: linoleum tile and low-pile carpet. These surfaces differ in characteristics and were intended to represent indoor surfaces commonly encountered in everyday MWC mobility.

### Component test results and discussion

The mass of the various casters were smaller than the mass of the drive wheels by about an order of magnitude, with casters ranging between 0.12 and 0.39 kg and drive wheels ranging between 1.71 and 2.07 kg (Tables 1 and 2). Within casters, the heaviest was 0.27 kg (5 x 1.5" Primo SR), or 225% greater in mass than the lightest (3 x 1" FLNC). Within drive wheels, the heaviest, Solid Mag, was 0.36 kg (21%) greater in mass than the lightest, Spinergy. However, when comparing these components to the overall mass of the MWC system (approximated as 100 kg), the drive wheels and casters each only account, at most, 4% and 0.8% of the system mass, respectively, indicating that the benefits gained from a lighter caster or drive wheel are minute.

**Table 1.** Caster wheel properties.

| Name | Caster wheel | Diameter [cm] | Tire width [cm] | Mass [kg] | Tire hardness |
|---|---|---|---|---|---|
| 3 x 1" Frog Legs Narrow Court (FLNC) |  | 7.6 | 2.5 | 0.12 | 88 |
| 4 x 1.5" Frog Legs Soft Roll (FLSR) |  | 10.6 | 3.6 | 0.22 | 76 |
| 5 x 1.5" Primo Soft Roll (SR) |  | 12.6 | 2.2 | 0.39 | 65 |
| 5 x 1" Primo |  | 12.4 | 2.4 | 0.22 | 85 |
| 6 x 1" Primo Pneumatic (35 psi inflation) |  | 15.1 | 2.8 | 0.26 | 60 |
| 6 x 1" Primo |  | 14.4 | 2.6 | 0.30 | 89 |
| 6 x 1" Frog Legs Narrow Court (FLNC) |  | 15.2 | 2.5 | 0.31 | 89 |
| 6 x 1.5" Primo |  | 14.7 | 3.7 | 0.33 | 89 |

**Table 2.** Drive wheel properties.

| Name | Drive wheel | Diameter [cm] | Tire width [cm] | Mass [kg] | Tire hardness |
|---|---|---|---|---|---|
| 24 x 1" Solid Mag |  | 62 | 2.75 | 2.07 | 82 |
| 24 x 1" Spinergy with Schwalbe Marathon Plus tires (100 psi inflation) |  | 60 | 2.65 | 1.71 | 49 |
| 24 x 1" Schwalbe Right Run (100 psi inflation) |  | 60 | 2.85 | 1.82 | 62 |
| 24 x 1-3/8" Primo Orion Standard Pneumatic (75 psi inflation) |  | 62 | 3.28 | 1.86 | 67 |
| 24 x 1-3/8" Primo VTrak (65 psi inflation) |  | 62 | 3.24 | 1.94 | 65 |
| 24 x 1-3/8" Primo XPress |  | 60 | 2.90 | 2.06 | 77 |

## Caster Wheels

3 x 1″ FLNC

4 x 1.5″ FLSR

5 x 1″ Primo

5 x 1″ Primo SR

6 x 1″ FLNC

6 x 1″ Primo

6 x 1″ Primo Pneumatic

6 x 1.5″ Primo

## Drive Wheels

Solid Mag

Spinergy

Schwalbe Right Run

Std Pneumatic

Primo VTrak

Primo XPress

**Figure 5.** Tire profiles.

**Table 3.** Component loadings by representative system weight-distribution.

| Percent load on drive wheels (Total load = 100 kg) | Normal load on each caster | Normal load on each drive wheel |
|---|---|---|
| 60% | 20 kg | 30 kg |
| 70% | 15 kg | 35 kg |
| 80% | 10 kg | 40 kg |

### Rolling resistance

The rolling resistances of casters and drive wheels under each configuration load are tabulated in Table 4 (tile) and Table 5 (carpet). The linear regressions of rolling resistances, $R^2 \geq 0.95$, suggest that the regression slope is a suitable metric of component load sensitivity. Load sensitivity is a parameter reflecting the relative increase in rolling resistance and scrub torque as a function of applied load. Plots of rolling resistance versus load for casters and drive wheels on tile and carpet can be found in the Supplemental Materials.

For casters on tile, the rolling resistance average across all three loads ranged from 1.16 N (4 x 1.5″ FLSR) to 2.55 N (6 x 1″

**Table 4.** Caster and drive wheel rolling resistance forces (N) on tile.
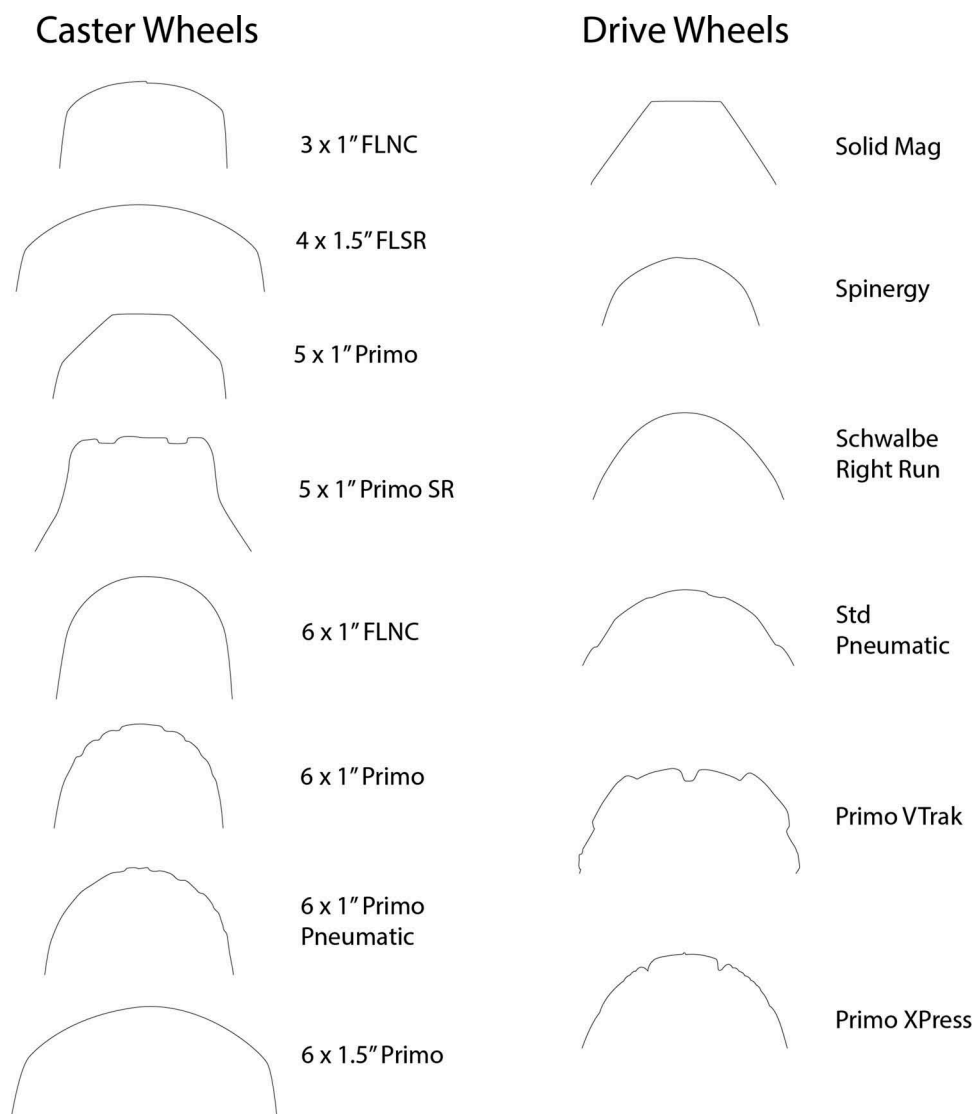
| | Caster load (kg) | | | | Linear regression | |
|---|---|---|---|---|---|---|
| Caster | 20 | 15 | 10 | Avg | Slope | $R^2$ |
| 4 x 1.5″ FLSR | 1.69 | 1.14 | 0.64 | 1.16 | 0.212 | 1.00 |
| 6 x 1″ FLNC | 1.70 | 1.20 | 0.70 | 1.20 | 0.166 | 1.00 |
| 6 x 1″ Primo | 2.07 | 1.52 | 0.96 | 1.52 | 0.154 | 1.00 |
| 5 x 1″ Primo | 2.39 | 1.64 | 0.93 | 1.65 | 0.152 | 1.00 |
| 3 x 1″ FLNC | 2.44 | 1.67 | 0.92 | 1.68 | 0.146 | 1.00 |
| 6 x 1.5″ Primo | 2.63 | 1.82 | 1.09 | 1.85 | 0.110 | 1.00 |
| 5 x 1.5″ Primo SR | 2.83 | 1.98 | 1.17 | 1.99 | 0.100 | 1.00 |
| 6 x 1″ Pneumatic | 3.60 | 2.59 | 1.47 | 2.55 | 0.106 | 1.00 |

| | DW load (kg) | | | | Linear regression | |
|---|---|---|---|---|---|---|
| Drive wheel | 30 | 35 | 40 | Avg | Slope | $R^2$ |
| 24 x 1-3/8″ Primo VTRAK | 0.50 | 0.90 | 1.46 | 0.95 | 0.193 | 1.00 |
| 24 x 1-3/8″ Std Pneumatic | 0.53 | 1.13 | 1.36 | 1.01 | 0.092 | 1.00 |
| 24 x 1″ Schwalbe Right Run | 1.12 | 1.48 | 1.71 | 1.44 | 0.083 | 0.94 |
| 24 x 1″ Spinergy | 1.07 | 1.58 | 1.99 | 1.55 | 0.059 | 0.99 |
| 24 x 1 3/8″ Primo XPRESS | 1.60 | 2.08 | 3.04 | 2.24 | 0.144 | 0.97 |
| 24 x 1″ Solid Mag | 3.61 | 4.57 | 5.53 | 4.57 | 0.096 | 0.99 |

Pneumatic), reflecting a 121% increase in average rolling resistance. For drive wheels on tile, the average rolling resistance, across all three loads, ranged from 0.95 N (Primo VTRAK) to 4.57 N (Solid Mag), reflecting a 135% increase in rolling resistance.

**Table 5.** Caster and drive wheel rolling resistance forces (N) on carpet.

| Caster | Caster load (kg) | | | | Linear regression | |
|---|---|---|---|---|---|---|
| | 20 | 15 | 10 | Avg | Slope | $R^2$ |
| 6 x 1" Pneumatic | 5.95 | 4.37 | 2.97 | 4.43 | 0.298 | 1.00 |
| 4 x 1.5" FLSR | 6.33 | 4.96 | 3.34 | 4.88 | 0.354 | 1.00 |
| 5 x 1" Primo | 6.41 | 4.91 | 3.38 | 4.90 | 0.349 | 1.00 |
| 5 x 1.5" Primo SR | 7.03 | 5.16 | 3.48 | 5.22 | 0.519 | 0.99 |
| 6 x 1.5" Primo | 7.22 | 5.40 | 3.73 | 5.45 | 0.303 | 1.00 |
| 6 x 1" FLNC | 8.02 | 5.92 | 4.24 | 6.06 | 0.405 | 0.99 |
| 6 x 1" Primo | 8.50 | 6.73 | 4.45 | 6.56 | 0.378 | 1.00 |
| 3 x 1" FLNC | 10.82 | 7.80 | 5.63 | 8.08 | 0.299 | 1.00 |
| Drive wheel | DW load (kg) | | | | Linear regression | |
| | 30 | 35 | 40 | Avg | Slope | $R^2$ |
| 24 x 1-3/8" Std Pneumatic | 2.35 | 3.28 | 4.19 | 3.27 | 0.321 | 0.98 |
| 24 x 1-3/8" Primo VTRAK | 2.82 | 3.42 | 4.47 | 3.57 | 0.162 | 1.00 |
| 24 x 1" Spinergy | 3.36 | 4.15 | 4.98 | 4.16 | 0.184 | 1.00 |
| 24 x 1" Schwalbe Right Run | 3.44 | 4.41 | 5.04 | 4.30 | 0.160 | 0.99 |
| 24 x 1 3/8" Primo XPRESS | 2.89 | 5.37 | 6.45 | 4.90 | 0.356 | 0.95 |
| 24 x 1" Solid Mag | 5.25 | 7.25 | 8.46 | 6.99 | 0.165 | 0.98 |

**Table 7.** Caster and drive wheel scrub torques (Nm) on carpet.

| Caster | Caster load (kg) | | | | Linear regression | |
|---|---|---|---|---|---|---|
| | 20 | 15 | 10 | Avg | Slope | $R^2$ |
| 3 x 1" FLNC | 1.13 | 0.89 | 0.51 | 0.84 | 0.062 | 0.98 |
| 5 x 1" Primo | 1.36 | 0.96 | 0.59 | 0.97 | 0.077 | 1.00 |
| 6 x 1.5" Primo | 1.45 | 0.97 | 0.54 | 0.99 | 0.091 | 1.00 |
| 6 x 1" Primo | 1.47 | 1.09 | 0.63 | 1.07 | 0.084 | 1.00 |
| 6 x 1" FLNC | 1.46 | 1.17 | 0.69 | 1.11 | 0.077 | 0.98 |
| 4 x 1.5" FLSR | 1.71 | 1.31 | 0.78 | 1.27 | 0.093 | 0.99 |
| 5 x 1.5" Primo SR | 1.78 | 1.41 | 0.86 | 1.35 | 0.092 | 0.99 |
| 6 x 1" Pneumatic | 2.60 | 1.77 | 1.22 | 1.86 | 0.138 | 0.99 |
| Drive wheel | DW load (kg) | | | | Linear regression | |
| | 30 | 35 | 40 | Avg | Slope | $R^2$ |
| 24 x 1 3/8" Primo XPRESS | 1.85 | 2.21 | 2.59 | 2.22 | 0.073 | 1.00 |
| 24 x 1-3/8" Std Pneumatic | 4.57 | 5.15 | 5.72 | 5.15 | 0.114 | 1.00 |
| 24 x 1" Solid Mag | 4.19 | 5.04 | 6.45 | 5.23 | 0.226 | 0.98 |
| 24 x 1-3/8" Primo VTRAK | 5.67 | 6.65 | 7.88 | 6.74 | 0.221 | 1.00 |
| 24 x 1" Schwalbe Right Run | 5.92 | 6.71 | 7.98 | 6.87 | 0.206 | 0.98 |
| 24 x 1" Spinergy | 6.45 | 7.29 | 8.40 | 7.38 | 0.195 | 0.99 |

For casters on carpet, the rolling resistance, averaged across all three loads, ranged from 4.47 (6 x 1" Pneumatic) to 7.97 N (3 x 1" FLNC), a 82% increase. For drive wheels on carpet, the rolling resistance, averaged across all three loads, ranged from 3.27 (Std Pneumatic) to 6.99 N (Solid Mag), a 121% increase.

The coefficients of variation (COVs) of the rolling resistance tests on tile ranged from 1% to 6% across the cohort of drive wheels and casters, indicating low variance across the trials. On carpet the COVs span 2–9%, which suggests the test method is repeatable on a surface with greater energy loss. Complete tabulated COV values can be found in the Supplemental Information.

### Scrub torque

The scrub torques of casters and drive wheels on tile and carpet are tabulated in Tables 6 and 7, respectively, along with the results of the applied linear regression. All tires exhibited an $R^2 \geq 0.98$ except for the Schwalbe Right Run, which had the lowest slope and an $R^2 = 0.79$.

For casters on tile, the scrub torque average across all three loads ranged from 0.52 to 1.99 Nm, with the lowest being the 3 x 1" FLNC and the highest being the 6 x 1" Pneumatic,

**Table 6.** Caster and drive wheel scrub torques (Nm) on tile.

| Caster | Caster load (kg) | | | | Linear regression | |
|---|---|---|---|---|---|---|
| | 20 | 15 | 10 | Avg | Slope | $R^2$ |
| 3 x 1" FLNC | 0.72 | 0.53 | 0.32 | 0.52 | 0.040 | 1.00 |
| 6 x 1.5" Primo | 0.87 | 0.61 | 0.32 | 0.60 | 0.055 | 1.00 |
| 6 x 1" FLNC | 0.90 | 0.62 | 0.30 | 0.61 | 0.059 | 1.00 |
| 5 x 1" Primo | 0.91 | 0.64 | 0.41 | 0.66 | 0.050 | 1.00 |
| 6 x 1" Primo | 1.32 | 0.93 | 0.50 | 0.92 | 0.083 | 1.00 |
| 4 x 1.5" FLSR | 1.70 | 1.10 | 0.64 | 1.15 | 0.107 | 0.99 |
| 5 x 1.5" Primo SR | 1.72 | 1.28 | 0.86 | 1.29 | 0.086 | 1.00 |
| 6 x 1" Pneumatic | 2.94 | 2.02 | 1.00 | 1.99 | 0.194 | 1.00 |
| Drive wheel | DW load (kg) | | | | Linear regression | |
| | 30 | 35 | 40 | Avg | Slope | $R^2$ |
| 24 x 1 3/8" Primo XPRESS | 2.16 | 2.81 | 3.82 | 2.93 | 0.166 | 0.98 |
| 24 x 1" Solid Mag | 2.78 | 3.60 | 4.17 | 3.52 | 0.140 | 0.99 |
| 24 x 1" Schwalbe Right Run | 3.77 | 3.82 | 4.72 | 4.10 | 0.094 | 0.79 |
| 24 x 1" Spinergy | 4.74 | 5.36 | 6.34 | 5.48 | 0.160 | 0.98 |
| 24 x 1-3/8" Std Pneumatic | 5.16 | 6.19 | 7.24 | 6.20 | 0.208 | 1.00 |
| 24 x 1-3/8" Primo VTRAK | 5.41 | 6.36 | 7.50 | 6.42 | 0.209 | 1.00 |

reflecting a 278% increase. For drive wheels on tile, the scrub torque average across all three loads ranged from 2.93 to 6.42 Nm, with the lowest being the Primo XPRESS and the highest being the Primo VTRAK, reflecting a 111% increase. For casters on carpet, the scrub torque average across all three loads ranged from 0.84 to 1.86 Nm, with the lowest being the 3 x 1" FLNC and the highest being the 6 x 1" Pneumatic, a 121% increase. For drive wheels on carpet, the scrub torque average across all three loads ranged from 2.22 to 7.38 Nm, with the lowest being the Primo XPRESS and the highest being the Spinergy, a 233% increase.

Comparing the tile scrub torques of casters and drive wheels, all drive wheels exhibit markedly greater scrub torques than the casters and exhibit a greater slope compared to all casters except the 6 x 1" Pneumatic.

The COVs across drive wheels and casters ranged from 0% to 8% for tile and 0–12% for carpet. The 24 x 1" Mag on carpet demonstrated the highest variance; options that may reduce variance include adding another conditioning trial or adding additional test trails. Complete tabulated COV values can be found in the Supplemental Information.

### Discussion

Test method validation was assessed using design criteria, accuracy, linearity, repeatability, and sensitivity. The test methods were able to meet the design criteria of being able to evaluate casters and drive wheels, over different surfaces and loads. For the rolling resistance test method, validation was assessed using accuracy of the instrumentation, linearity of the measured wheel velocities, and repeatability of the output. For the scrub test method, validation assessment included accuracy of the applied load and repeatability of the scrub torque. Both test methods demonstrated sensitivity to change to applied load, surface and component.

The described test methods were sensitive in measuring differences in energy loss of both casters and drive wheels on carpet and tile. On tile, caster rolling resistances increased 120% and drive wheel rolling resistance increased 135% when comparing the tires with the lowest to highest values. On carpet, the increases were 82% for casters and 121% for

drive wheels. Scrub torque differences were even more pro-found. On tile, the differences between casters were 278% and drive wheel differences were 111% and on carpet, the differences in casters and drive wheels were 121% and 232%, respectively. These differences in components are significant, because they represent the ranges of energy dissipated during MWC maneuvers. The user must overcome this energy loss with every propulsion stroke.

The caster rolling resistance data on tile present trends that both corroborate and conflict with the findings of prior assessments of rolling resistance. Rolling resistance forces fall within the same range found by Sauret (Sauret et al., 2012), but casters do not follow the trend of greater rolling resistance with decreasing diameter. This may be explained by this study's smaller sample of components, which vary not only in diameter but also in tire width, profile, and hardness. All of these factors influence wheel contact surface which, in turn, influences rolling resistance (Kauzlarich & Thacker, 1985). Within the DW data, the two solid tires, the Primo XPRESS and Solid Mag, have greater rolling resistances compared to the pneumatic drive wheels, with the Solid Mag values especially pronounced (Tables 4 and 5). This result matches well with the findings of a dynamometer-based rolling resistance study (Kwarciak et al., 2009), which found that the solid tires exhibited rolling resistances of 4–9 N while pneumatic tires exhibited rolling resistances of 2–3 N. The differences between their presented values and ours are likely due to their use of a dynamometer versus over-ground motion and due to the different contact surfaces.

For casters, the relative rankings of rolling resistance illustrate disparate performance on tile versus carpet. While the 4 × 1.5" FLSR exhibited low rolling resistances on both surfaces, the 6 x 1" pneumatic caster went from the lowest rolling resistance on tile to the greatest rolling

resistance on carpet. The relative rankings of DW rolling resistance were fairly consistent on tile and carpet. On both surfaces, the Primo VTRAK and Std Pneumatic exhibited low rolling resistances whereas the Primo XPRESS and Solid Mag exhibited high rolling resistances. When considering scrub torque, the relative rankings were more consistent with casters compared to drive wheels when comparing surfaces. While some ordering was apparent at the lower scrub torque range, the 5 × 1.5" Primo SR and 6 x 1" pneumatic casters exhibited the greatest scrub torques on both tile and carpet. Relative drive wheel scrub torques exhibited more disparity across surfaces. The Std Pneumatic tire went from the second highest torque on tile to the second lowest torque on carpet.

Caster and DW sensitivity to load is defined by the relative increase in energy loss with increasing load and is reflected in the slopes of the regression lines (Tables 4–7). For casters, a greater separation in rolling resistance and scrub torque is evident at the higher loads on both surfaces. This suggests that when a MWC is configured with a low weight distribution on the casters (e.g. with 80% load on drive wheels), caster selection does not significantly impact rolling resistance or scrub torque. However, when the caster accepts more load (i.e., 60% load on drive wheels), the selection of casters is more important and may significantly affect the user effort, especially on carpet. The load sensitivities of the drive wheels tend to be greater than that of the casters, most likely, due to the greater loads. For both rolling resistance and scrub, a separation between drive wheels exists at all loads. Prior research suggests that shifting more load onto the drive wheels is the most effective means of reducing overall wheelchair rolling and turning resistance (Lin et al., 2015; Sauret et al., 2012).
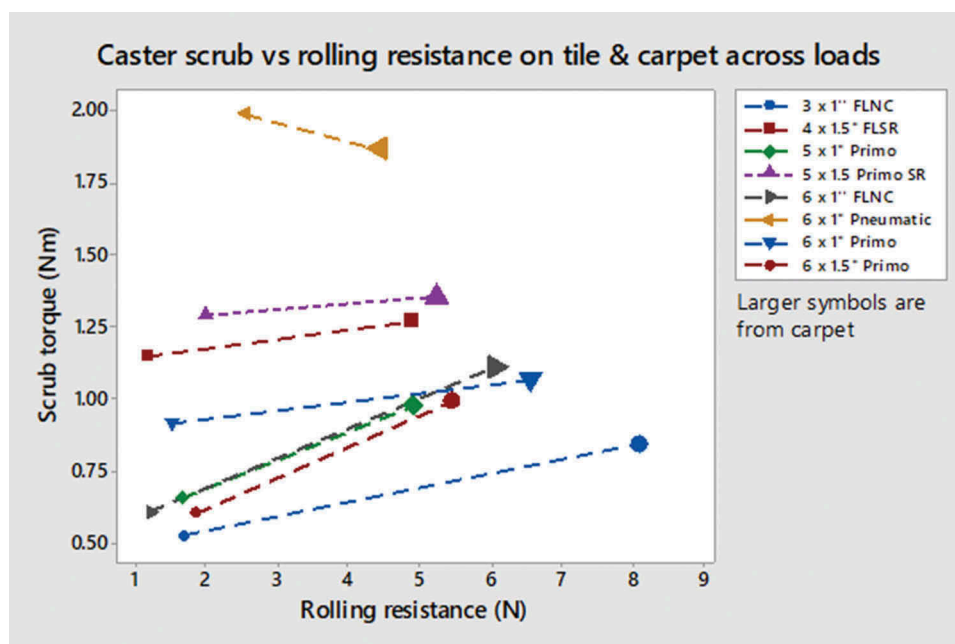


**Figure 6.** Caster scrub torque versus rolling resistance across loads and surfaces.
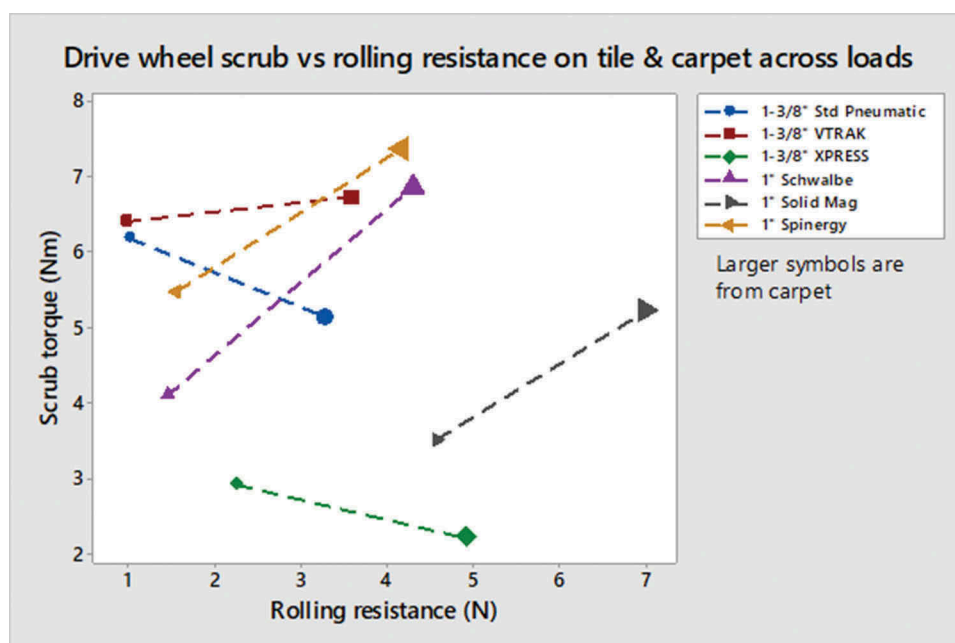
**Figure 7.** Drive wheel scrub torque versus rolling resistance across loads and surfaces.

## Combined analysis

Assessing performance of components in both rolling resistance and scrub torque offers a fuller picture of the complexity of documenting energy loss and demonstrates the tradeoffs between managing both these sources of energy loss. Figures 6 and 7 plot the rolling resistance versus scrub, averaged across loads, on tile and carpet. The 6 x 1" pneumatic caster has the greatest scrub torque on both surfaces and highest tile rolling resistance but the lowest rolling resistance on carpet. The 6 x 1" FLNC has the best balance on tile as evidenced by its low rolling resistance and scrub torque, but has a relatively high rolling resistance on carpet. Overall, the 5 x 1" and 6 × 1.5" Primo casters appear to offer the best overall balance in energy loss performance across loads and surfaces.

For the DWs, the Solid Mag has the lowest scrub torque but the highest rolling resistance on both surfaces. The Std Pneumatic and VTRAK offer similar combined energy losses on tile with a low rolling resistance but relatively high scrub torque, but the Std Pneumatic performs better on carpet as indicated by its lower in scrub torque. Spinergy with Schwalbe Marathon Plus tire and Schwalbe Right Run have very similar resistive losses across both surfaces. On tile, they are quite balanced with low rolling resistances and moderate scrub torques, but on carpet, they exhibit the highest scrub torques. On tile, the 1 × 1 3/8" XPRESS and 1" Schwalbe Right Run tires reflected the most beneficial energy loss profiles. They offered a balance of relatively low rolling resistance and scrub torques, but when traveling on carpet, the XPRESS offers better combined performance. However, categorizing any tire as 'beneficial' comes with an important caveat that must be considered when assessing drive wheels. Rolling resistance is ever-present and impacts all maneuvers, both straight and turning, so a benefit exists in using a tire with low rolling

resistance on most surfaces. However, unlike casters, drive wheels must retain traction during everyday use to ensure safe maneuvering. Traction is embodied by energy loss and may be needed on certain surfaces and in turning situations. For example, a very low drive wheel scrub torque as embodied by the Primo XPRESS tires may negatively impact wheelchair traction during turning at relatively higher speeds which may result in sliding. Similarly, for persons needing traction while negotiating soft (e.g. sand) or wet surfaces, a tire with a more pronounced tread pattern may be advantageous even if it results in greater energy loss. A benefit would exist if wheelchair users were provided with a set of tires – one that has optimal performance indoors and on hard outdoor surfaces, and another that offers traction needed in inclement weather or when traveling on soft terrain. Assuming a single tire can perform equally well under all conditions and on all surfaces is a fallacy and is not reflected in car or bike tires, which are regularly chosen by their context of use.

## Limitations

The objective of this study was to develop and validate test methods to characterize energy loss in casters and drive wheels that reflect both straight and turning trajectories while able to assess different surfaces. Like all test methods, those described here have limitations. Coast-down rolling resistance requires space, defines a window of acceptable release velocity and the need to maintain a straight trajectory. As such, it comes with technical requirements that can result in failed trials that must be repeated. The use of reference casters simplifies the test method but reflects investigator decisions. While a 5" wheelchair caster was used in this test, one could select any wheel that offers the capability of affixing a variety of test wheels for analysis. The scrub torque test incorporates pure

rotation, which reflects the highest scrub torque but may not generalizable for all cases, i.e. energy losses incurred in turning over different radii of curvature. Since there would be no practical way to test an infinite number of turning radii, this test reflects a compromise in measurement to achieve a practical test method that can be deployed using a standard materials testing machine. The data presented here utilized a single conditioning trial which is consistent with ASTM tests. However, use of two conditioning trials should be considered to accommodate the variation that can occur with some surfaces and tires with the goal of reducing the coefficients of variation between trials. These test methods were then deployed on a small sample of components as a means to assess the test method's ability in distinguishing energy loss across components. While the results can be used to define the relative energy losses within the tested cohort, they cannot be used to position these components within the wide range of components used in manual wheelchairs. Furthermore, component testing is useful in assessing the mechanical performance of drive wheels and casters but cannot yet be used to directly state impact on the propulsion effort of an occupied wheelchair. Systems-level testing is needed to supplement component testing in order to document the influence of component energy losses on propulsion effort. Once this influence is defined, rolling resistance and scrub torque testing can then be used to inform the selection of drive wheels and casters during wheelchair prescriptions.

## Conclusion

Characterizing the energy loss of casters and drive wheels is important in understanding the differences in performance that have the potential to impact propulsion effort. Because maneuvering manual wheelchairs is embodied by different trajectories, assessing energy loss in straight and turning trajectories is needed. Moreover, the nature of manual wheelchairs and their use requires evaluation of energy loss over different surfaces and loads. The test methods defined in this study resulted in repeatable measurements of rolling resistance and scrub torque using two surfaces and three loading conditions. Because of the complex interactions between energy loss and surfaces, the results of these test methods can help choose components by reflecting on the context of use. For example, if a user regularly spends time on carpeted indoor surfaces, one can infer more maneuvering resulting in a greater importance of both scrub torque and rolling resistance on that surface. A wider deployment of these test methods, including assessment of other surfaces, may be useful in categorizing casters and drive wheels that have equivalent performance. By understanding equivalency in performance, clinicians and users will be better empowered to make informed decisions when configuring wheelchairs.

## Funding

## ORCID

Stephen Sprigle   http://orcid.org/0000-0003-0462-0138

## References

Bascou, J., Pillet, H., Kollia, K., Sauret, C., Thoreux, P., & Lavaste, F. (2014). Turning resistance of a manual wheelchair: A theoretical study. *Computer Methods in Biomechanics and Biomedical Engineering*, 17(sup1), 94–95. doi:10.1080/10255842.2014.931159

Bascou, J., Sauret, C., Villa, C., Lavaste F., & Pillet, H. (2015). Measurement of wheelchair adjustment effects on turning deceleration. *Computer Methods in Biomechanics and Biomedical Engineering*, 18(sup1), 1882–1883. doi:10.1080/10255842.2015.1075327

Brubaker, C. (1986). Wheelchair prescription: An analysis of factors that affect mobility and performance. *Journal of Rehabilitation Research and Development*, 23(4), 19–26.

Chan, F. H., Eshraghi, M., Alhazmi, M. A., & Sawatzky, B. J. (2018). The effect of caster types on global rolling resistance in manual wheelchairs on indoor and outdoor surfaces. *Assistive Technology*, 30(4), 176–182. doi:10.1080/10400435.2017.1307880

ASTM Standard D1349-14 A. (2014). *Standard practice for rubber – Standard conditions for testing*. West Conshohocken, PA: ASTM International. Retrieved from www.astm.org.

ASTM Standard E1337-90 A. (2012). *Standard test method for determining longitudinal peak braking coefficient of paved surfaces using standard reference test tire*. West Conshohocken, PA: ASTM International. Retrieved from www.astm.org.

Eicholtz, M. R., Caspall, J. J., Dao, P. V., Sprigle, S., & Ferri, A. (2012). Test method for empirically determining inertial properties of manual wheelchairs. *Journal of Rehabilitation Research and Development*, 49(1), 51–62. doi:10.1682/JRRD.2011.03.0045

Frank, T. G., & Abel, E. W. (1989). Measurement of the turning, rolling and obstacle resistance of wheelchair castor wheels. *Journal of Biomedical Engineering*, 11(6), 462–466. doi:10.1016/0141-5425(89)90040-X

Hoffman, M. D., Millet, G. Y., Hoch, A. Z., & Candau, R. B. (2003). Assessment of wheelchair drag resistance using a coasting deceleration technique. *American Journal of Physical Medicine & Rehabilitation*, 82(11), 880–889. doi:10.1097/01.PHM.0000091980.91666.58

Hofstad, M., & Patterson, P. E. (1994). Modelling the propulsion characteristics of a standard wheelchair. *Journal of Rehabilitation Research and Development*, 31(2), 129–137.

International Standards Organization. *Wheelchairs – Part 11: Test dummies*. ISO 7176-11:20122012.

Kauzlarich, J., Bruning, T., & Thacker, J. (1984). Wheelchair caster shimmy and turning resistance. *Journal of Rehabilitation Research and Development*, 21(2), 15–29.

Kauzlarich, J., & Thacker, J. G. (1985). Wheelchair tire rolling resistance and fatigue. *Journal of Rehabilitation Research and Development*, 22(3), 25–41. doi:10.1682/JRRD.1985.07.0025

Kwarciak, A. M., Yarossi, M., Ramanujam, A., Dyson-Hudson, T. A., & Sisto, S. A. (2009). Evaluation of wheelchair tire rolling resistance using dynamometer-based coast-down tests. *Journal of Rehabilitation Research and Development*, 46(7), 931–938. doi:10.1682/JRRD.2008.10.0137

Lin, J.-T., Huang, M., & Sprigle, S. (2015). Evaluation of wheelchair resistive forces during straight and turning trajectories across different wheelchair configurations using free-wheeling coast-down test. *Journal of Rehabilitation Research and Development*, 52(7), 763. doi:10.1682/JRRD.2014.10.0235

Lin, J.-T., & Sprigle, S. (2019). The influence of operator and wheelchair factors on wheelchair propulsion effort. *Disability and Rehabilitation: Assistive Technology*, 1–8. doi:10.1080/09638288.2019.1585972

Sauret, C., Bascou, J., de Saint Rémy, N., Pillet, H., Vaslin, P., & Lavaste, F. (2012). Assessment of field rolling resistance of manual wheelchairs. *Journal of Rehabilitation Research and Development*, 49(1), 63–74. doi:10.1682/JRRD.2011.03.0050

Sawatzky, B., Kim, W., & Denison, I. (2004). The ergonomics of different tyres and tyre pressure during wheelchair propulsion. *Ergonomics, 47*(14), 1475–1483. doi:10.1080/00140130412331290862

Silva, L., Corrêa, F., Eckert, J., Santiciolli, F., & Dedini, F. (2017). A lateral dynamics of a wheelchair: Identification and analysis of tire parameters. *Computer Methods in Biomechanics and Biomedical Engineering, 20*(3), 332–341. doi:10.1080/10255842.2016.1233327

Silva, L., Dedini, F., Corrêa, F., Eckert, J., & Becker, M. (2016). Measurement of wheelchair contact force with a low cost bench test. *Medical Engineering & Physics, 38*(2), 163–170. doi:10.1016/j.medengphy.2015.11.014

Sonenblum, S. E., & Sprigle, S. (2017). Wheelchair use in ultra-lightweight wheelchair users. *Disability and Rehabilitation: Assistive Technology, 12*(4), 396–401.

Sonenblum, S. E., Sprigle, S., & Lopez, R. A. (2012). Manual wheelchair use: Bouts of mobility in everyday life. *Rehabilitation Research and Practice, 2012,*1–7. doi: 10.1155/2012/753165.

Zepeda, R., Chan, F., & Sawatzky, B. (2016). The effect of caster wheel diameter and mass distribution on drag forces in manual wheelchairs. *Journal of Rehabilitation Research & Development, 53*(6), 893–900. doi:10.1682/JRRD.2015.05.0074